

Applications of Task-Based Image Quality Assessment in Nuclear Medicine Imaging

Eric C. Frey, Ph.D.

Division of Medical Imaging Physics
Russell H. Morgan Department of Radiology and
Radiological Science
Johns Hopkins University

Acknowledgements

- Organizers for inviting me
- Xin He, etc., at Johns Hopkins
- Mike King, Howard Gifford, etc., at U. Mass. Med.
- Jinyi Qi at U.C. Davis
- Paul Kinahan and coworkers at U. Wash.
- Gene Gindi and coworkers at Stony Brook

Scope of Talk

- Applications discussed limited to
 - SPECT and PET
 - Anthropomorphic Model Observers
 - No studies using purely human observers
 - No studies using ideal observers
 - Classification tasks
 - Detection
 - Detection + localization
 - Detection + characterization

Differences Between Slides and Handouts

- Fixed some typos
- Added some additional references
- The new slides will be available for download from:
 - <http://mirlbcc1.jhoc1.jhmi.edu/public>

Goals

- Describe choices that must be made to perform a task-based assessment
- Be as practical, detailed, and concrete as possible
- Give examples of applications of task-based assessment in range of nuclear medicine imaging applications
- Focus on methods rather than results

Outline

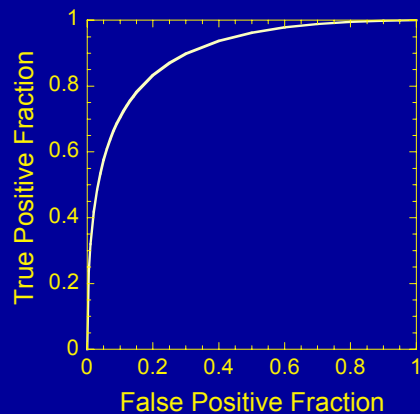
- Components of task-based assessment
 - Task models
 - Object model
 - Imaging system model
 - Observer model
 - Figure of merit (FOM)
- Examples of task-based assessment
 - Myocardial perfusion SPECT
 - Hepatic SPECT
 - Ga-67 SPECT
 - 2D vs. 3D PET tumor imaging
 - Optimization of MAP reconstruction for PET tumor imaging
- Summary

Task Models

- Detection
- Detection + Localization
- Detection + Characterization

Detection Task

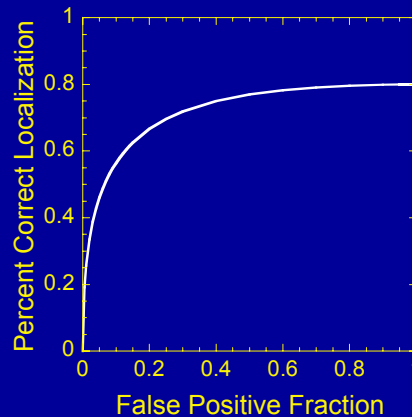
- Observer provides
 - Rating of confidence that signal is present anywhere in imageor
 - Rating of confidence that signal is present at a particular point in image (SPKE)
- Does not realistically model all clinical tasks
- Analyze using ROC analysis
- Figure of merit
 - Area under ROC curve (AUC)
 - Range: [0.5,1.0]



Metz C. E. 1978 Seminars in Nuclear Medicine

Detection+Localization Task

- Observer provides
 - Location of suspected signal
 - Rating of confidence that the signal is at this point
- Task may be more clinically realistic for some applications
- Analyze using LROC analysis
- Figure of Merit:
 - Area under LROC Curve (A_{LROC})
 - Range: [0,1]

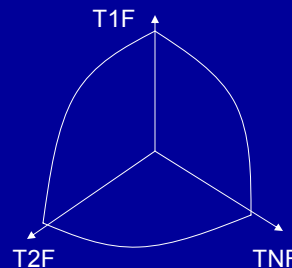
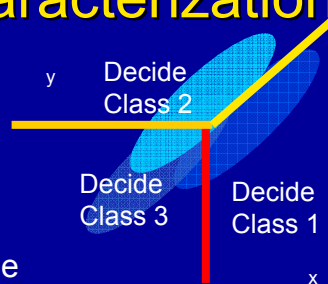


Swensson RG, Med Phys, 1996

Khurd and Gindi, IEEE Trans Med Imag 2005

Detection + Characterization

- Observer provides
 - Confidence rating that signal is present and class 1
 - Confidence rating that signal is present and class 2
- May be needed to model some clinical tasks
- Analyze using 3-class ROC analysis
- Figure of Merit
 - Volume under ROC surface (VUS)
 - Range [1/6, 1]



He, Metz, Links, Tsui, and Frey, IEEE Trans Med Imag, May, 2006

Outline

- Components of task-based assessment
 - Task models
 - **Object model**
 - Imaging system model
 - Observer model
 - Figure of merit (FOM)
- Examples of task-based assessment
 - Myocardial perfusion SPECT
 - Hepatic SPECT
 - Ga-67 SPECT
 - 2D vs. 3D PET tumor imaging
 - Optimization of MAP reconstruction for PET tumor imaging
- Summary

Object Model

- Background
 - Background known exactly (BKE)
 - Background known statistically (BKS)
- Signal
 - Signal known exactly (SKE)
 - Signal known statistically (SKS)

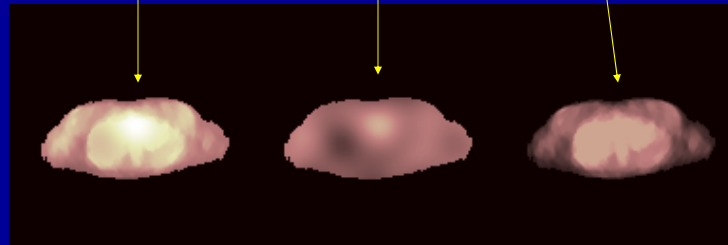
Background Models

- Background variability is essential
- Background variation should be as realistic as possible
- Ways to achieve this:
 - Statistically defined background
 - Single phantom, multiple signal locations
 - Collection (population of phantoms)

Statistically Defined Background

Lumpy Background

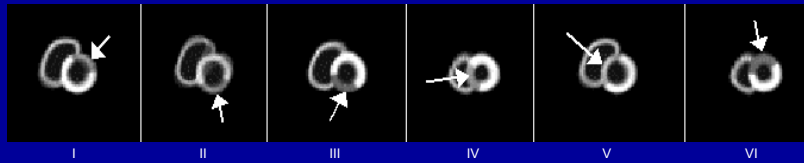
$$B = b \sum_{i=1}^K G(r_k, \sigma^2) + B_0$$



- Gaussian blobs with $\sigma^2 = 50$ (pixel²) at random locations r_k .
 - Number of blobs K is a Poisson r.v. with mean = 100.
 - $b = 150$.
- J. P. Rolland and H. H. Barrett, *J Opt Soc of Amer A*, 1992.
Qi, *IEEE Trans Nucl Sci*, 2006
- Courtesy of J.Y. Qi

Single Phantom Multiple Signal Locations

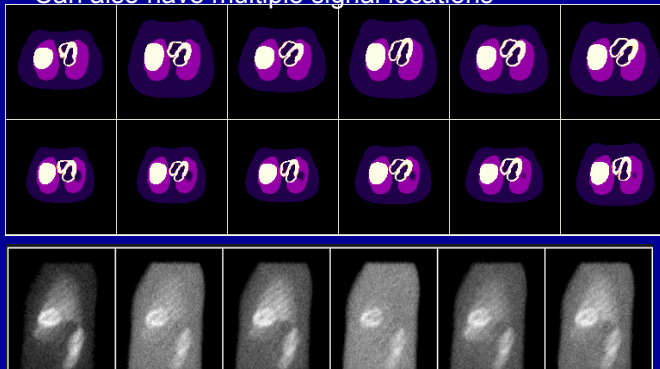
- Single heart and background
- Lesions at 6 locations



Frey et al. IEEE Trans Med Imaging, 2002

Multiple Phantoms

- NCAT Phantom
- 12 male, 12 female anatomies (females shown)
- Varied body, lung, liver and heart size, heart orientation
- Multiple randomly sampled organ uptakes for each anatomy
- Can also have multiple signal locations



He, Frey et al. IEEE Trans Nucl Sci 2004

Comparison of Background Definition Methods

- Statistically defined backgrounds
 - Easy to treat analytically
 - May not be sufficiently realistic for some applications
- Single phantom
 - Relatively simple to define object
 - Relatively easy to obtain projection data
 - Limited object variability
- Multiple phantoms
 - Substantial effort to define phantoms
 - Substantial effort to obtain projection images
 - Maximum realism

Types of Background

- Physical phantom
 - Accurate simulation of imaging system
 - Limited ability to model object variability
- Mathematical phantom (Frey, 2002; He, Frey, 2004)
 - May not model imaging system as well
 - Allows object variability limited only by computational resources
- Patient data (Gifford, TNS, 2001)
 - Most realistic model of object and imaging system
 - Object variability limited only by availability of patient data
 - Limited control over object parameters

Signal Models

- Signal Known Exactly (SKE)
 - Most model observers are derived for and optimal for this case (Barrett, 1993)
 - My not be useful for optimizing images for human use (Yendiki 2006)
- Variable size and contrast (He, Frey, 2004)
 - More realistic
 - Have been used successfully with model observers
- Signal shape depends on application
 - Myocardial perfusion defect limited to myocardium
 - Tumors approximated by sphere or 3D Gaussian

Outline

- Components of task-based assessment
 - Task models
 - Object model
 - **Imaging system model**
 - Observer model
 - Figure of merit (FOM)
- Examples of task-based assessment
 - Myocardial perfusion SPECT
 - Hepatic SPECT
 - Ga-67 SPECT
 - 2D vs. 3D PET tumor imaging
 - Optimization of MAP reconstruction for PET tumor imaging
- Summary

Modeling the Imaging System

- Must realistically model imaging system
 - To test attenuation compensation, model attenuation accurately and include approximate scatter model
 - To test approximate scatter compensation, use more accurate (e.g., Monte Carlo) scatter simulation
- Should model continuous nature of activity distribution
 - E.g., simulate using pixelized phantoms with pixel size $< \frac{1}{2}$ the size of projection bins

Components of Task Based Assessment Studies

- Task models
- Object model
- Imaging system model
- Observer model
- Figure of merit (FOM)

Imaging System Models

- Analytic simulation
 - Very computationally efficient
 - Hard to accurately model some physical processes (e.g., scatter in object and detector)
- Monte Carlo simulation
 - Can achieve high level of realism
 - Allows testing instrument designs without building them
 - Very computationally intensive
 - May need to combine analytic models for some parts of system with improve efficiency (e.g. X. Song, PMB, 2005)
- Physical Measurement (e.g. Chen, 2nd Biannual Workshop on Small-Animal SPECT Imaging, 2006)
 - Ultimate in accuracy
 - Hard to acquire large number of realizations
 - Requires access to real imaging system
 - Limited to physical phantoms and patients
- Hybrid (e.g. Gifford, TNS, 2001)
 - Physical measurement for background
 - Monte Carlo or analytic simulation of lesion

Outline

- Components of task-based assessment
 - Task models
 - Object model
 - Imaging system model
 - **Observer model**
 - Figure of merit (FOM)
- Examples of task-based assessment
 - Myocardial perfusion SPECT
 - Hepatic SPECT
 - Ga-67 SPECT
 - 2D vs. 3D PET tumor imaging
 - Optimization of MAP reconstruction for PET tumor imaging
- Summary

Model (Mathematical) Observers

- Most anthropomorphic observers are linear
- Dot product of observer template and image plus internal noise gives test statistic (analogous to rating value)
- Internal noise models variability of human observers
- Use channel model to better model human observers
- Addition of non-linear components to Hotelling observer (Zhang, Pham and Eckstein, TMI, 2006)

$$\lambda = \vec{h}^T \mathbf{M} \vec{g} + \tilde{n}$$

Scalar Test Statistic λ
 mxn Channel Matrix \mathbf{M}
 nx1 image vector \vec{g}
 mx1 Template Vector \vec{h}
 mx1 feature vector \vec{g}
 Internal noise \tilde{n}

Barrett, 1993

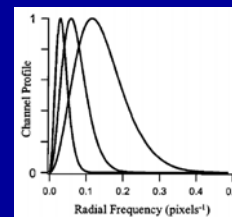
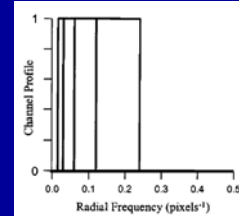
Abbey and Barrett, JOSA, 2001

Commonly Used Model Observers

- Channelized Non-Prewhitening Observer (CNPWO)
 - Simpler to implement than CHO
 - Template is simply the signal
 - Good agreement in several studies
- Channelized Hotelling Observer
 - Models ability of human observers to adapt to noise
 - Used in a large number of Nuclear Medicine related studies
 - Generally good agreement with human observer study results

Channel Shape

- Constant Q (SQR) Channels (e.g., Frey, 2002)
 - Non-overlapping
 - Used in many studies
 - Generally good agreement
- Difference of Gaussians (DOG) (Gifford and King, 2000)
 - Channels overlap
 - Used in fewer studies
 - To date, no significant advantage in predicting human observer performance compared to SQR channels



Channel Properties

- Should have zero response at 0 frequency
- Start channel can be important parameter that may need to be optimized for good agreement with human observers
- Bandwidth for n-th channel typically proportional to 2^n
- Number of channels
 - Typically 3-5
 - More channels increases difficulty of estimating observer
 - Depends on image size
 - Chosen based on relative size of noise and signal
- Shifted to suspected signal location

Observer Internal Noise

- Can improve absolute agreement between model observers and human observers
- Generally not needed when only rankings of methods are important

Abbey and Barrett, JOSA, 2001

Estimating the CHO Template

- CHO template is a function of the mean and covariances of the images after application of the channel model

$$\vec{h}^T = \left(\langle \overline{\mathbf{M}g_1} \rangle - \langle \overline{\mathbf{M}g_2} \rangle \right)^T (P\mathbf{C}_1 + P_2\mathbf{C}_2)^{-1}$$

CHO Template Vector \vec{h}^T
 Mean of Images belonging to class 1 and 2 after application of channel model $\langle \overline{\mathbf{M}g_1} \rangle - \langle \overline{\mathbf{M}g_2} \rangle$
 mxm Covariance matrices of images belonging to to classes 1 and 2 after application of channel model $\mathbf{C}_1, \mathbf{C}_2$
 Class 1 and 2 Prevalences P, P_2
 Matrix Inverse $(P\mathbf{C}_1 + P_2\mathbf{C}_2)^{-1}$

Analytic Estimation of CHO Template

- See J.Y. Qi, 2004 and Khurd, 2005c
- Extremely fast (1000x faster than ensemble methods)
- Based on estimates of mean and covariance at convergence
- Are approximate (but good approximation)
- Does not work for all algorithms (e.g., OS-EM)
- Does not allow modeling of non-linear processes

Monte Carlo Estimation of the CHO Template

- Simple to implement
 - Use sampling techniques to generate many sample images
 - Compute requisite mean and covariance matrices
- Completely general
 - Applicable to any background model
 - Applicable to any image processing (even nonlinear)
- Requires large number of images
 - Minimum of $\sim 4x$ number of elements in covariance matrix
 - Typically use several hundred samples
 - Large computation (weeks of CPU time) and storage demands (100s of GB of disk space)

Outline

- Components of task-based assessment
 - Task models
 - Object model
 - Imaging system model
 - Observer model
 - **Figure of merit (FOM)**
- Examples of task-based assessment
 - Myocardial perfusion SPECT
 - Hepatic SPECT
 - Ga-67 SPECT
 - 2D vs. 3D PET tumor imaging
 - Optimization of MAP reconstruction for PET tumor imaging
- Summary

Figures of Merit

- Detection Task
 - CHO SNR
 - Detectability (d_A)
 - Area under ROC curve (AUC)
- Detection+Localization
 - Area under LROC Curve (A_{LROC})
- Detection+Characterization
 - Volume under ROC Surface (VUS)

Relationships between Detection Task FOMs

- SNR is given by:
- If test statistics for two classes $\{\lambda_1\}$ and $\{\lambda_2\}$ are independent and Gaussian distributed, then $d_A = \text{SNR}$
- AUC and d_A are monotonically related

Means of test statistics from classes 1 and 2

$$\text{SNR}^2 = \frac{(\bar{\lambda}_1 - \bar{\lambda}_2)^2}{(\sigma_{\lambda_1}^2 + \sigma_{\lambda_2}^2)}$$

Variations of test statistics from classes 1 and 2

Analytic Estimation of FOMs

- Analytic expressions are available for SNR (J.Y. Qi 2004, 2006)
- Rapid estimation of A_{LROC} is available (Khurd 2005c)
- Expressions are approximate (but very good)
- Do not provide ROC or LROC curves
- Are related to AUC only if test statistics are independent and Gaussian distributed

Monte Carlo Estimation of FOMs

- Apply CHO template to ensemble of images to obtain ensemble of test statistics

Then

- Compute means and variances needed to compute SNR

or

- Analyze test statistics using codes (e.g., LABROC, CLABROC) for analyzing estimating the ROC or LROC Curve and AUC or A_{LROC}
- Take advantage of extensive statistical machinery developed for analyzing human observer data

Outline

- Components of task-based assessment
 - Task models
 - Object model
 - Imaging system model
 - Observer model
 - Figure of merit (FOM)
- Examples of task-based assessment
 - Myocardial perfusion SPECT
 - Hepatic SPECT
 - Ga-67 SPECT
 - 2D vs. 3D PET tumor imaging
 - Optimization of MAP reconstruction for PET tumor imaging
- Summary

Example 1

Myocardial Perfusion SPECT

- Frey 2002, Sankarin 2002, He 2004, Narayanan 2002
- Task
 - Myocardial defect detection
 - Signal position known exactly (ROC task)
- Questions
 - What is optimal number of iterations?
 - What is optimal combination of compensations?
 - What is optimal number of iterations?
 - What is optimal orbit (180 or 360°)?
 - Can acquisition time be reduced?

Object Models

- | | |
|---|---|
| <ul style="list-style-type: none">• MCAT Phantom population<ul style="list-style-type: none">– 24 anatomies<ul style="list-style-type: none">• 8 male flat diaphragm• 8 male w/raised diaphragm• 8 female– Constant heart size, shape and orientation– Organ size and shape varied with phantom– Constant organ activity concentration ratios– 6 defect locations, each with constant size– 12% defect contrast– 1/8 clinical count level | <ul style="list-style-type: none">• NCAT Phantom population<ul style="list-style-type: none">– 24 anatomies<ul style="list-style-type: none">• 12 male• 12 female– Randomly varied heart size, shape, and orientation– Randomly varied organ sizes and shapes– Randomly varied organ activities concentration ratios– 6 defect locations, size varied by +/- 25%– Defect contrast varied from 10-35%– Clinical count level |
|---|---|

Imaging System Model

- MCAT Phantom Study
 - Analytical simulation
 - Simulation voxel size was $\frac{1}{2}$ of reconstructed voxel size
- NCAT Phantom Study
 - Monte Carlo simulation
 - Simulation voxel size was $\frac{1}{2}$ of reconstructed voxel size

Observer Model

- CHO
- Applied to 32x32 short axis slices
- 4 SQR channels
 - Start freq and freq width of first channel= $1/64$ pixel⁻¹
- Ensemble estimation of template (training) using 864 images
- Internal noise not included

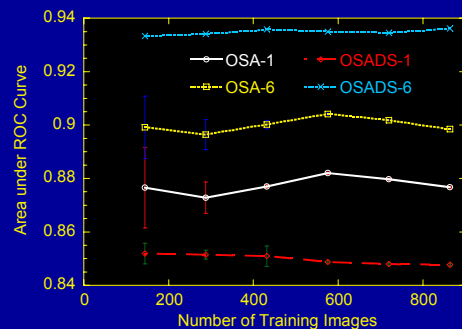
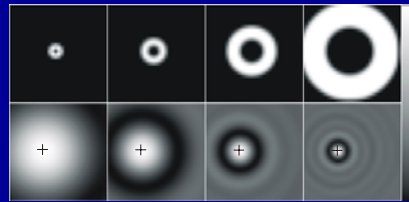
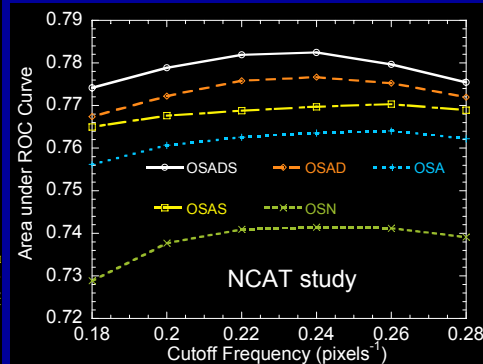
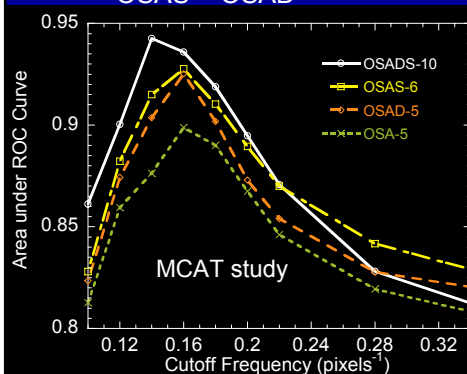


Figure of Merit

- Area under ROC Curve
- Estimated using CLABROC program from Metz et al
- Ensemble of testing images equal to # of training images (864)
- Tested for statistical significance of differences using CLABROC (takes into account correlations due to use of same data ensemble for all data treatments)

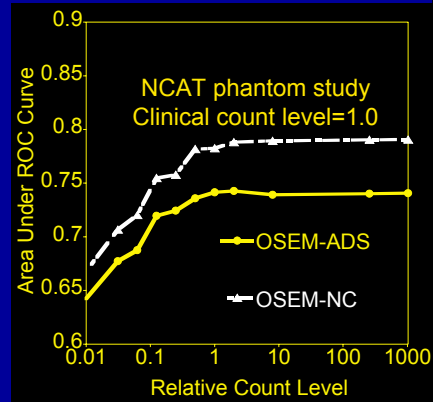
Results Reconstruction Parameters

- For MCAT study:
 - AUC much larger (despite 1/8 count level and lower contrast)
 - Optimal cutoff frequency much lower and sharper
 - Optimal number of iterations was larger
 - OSAS > OSAD



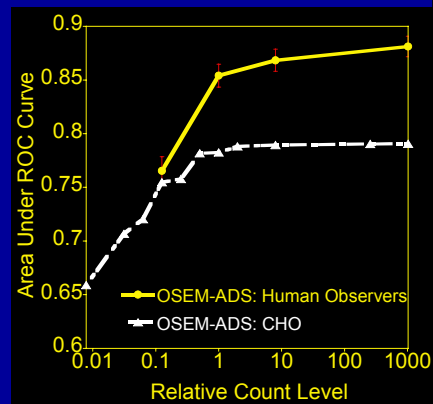
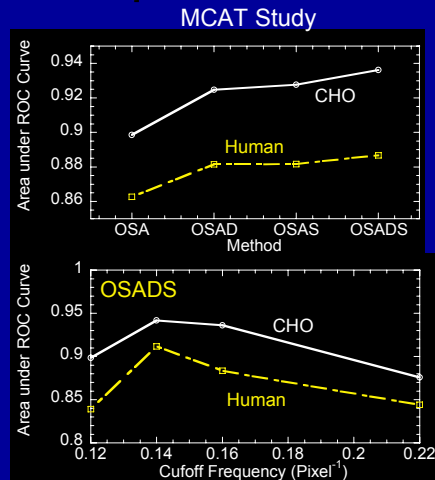
Results Effect of Count Level

- Demonstrates tradeoff between anatomical noise and statistical noise
 - Low count level: performance decreases with increasing noise
 - High count level: performance relatively constant
 - Very high count level: performance not perfect due to anatomical noise



Including realistic levels of object variation is essential!

Results Comparison w/ Human Observers

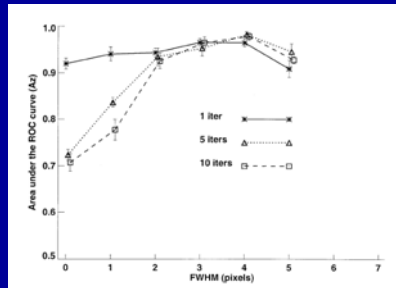


Correlation coef for AUCs: 0.904
Correlation coef for rankings: 0.964
CHO performed better than human

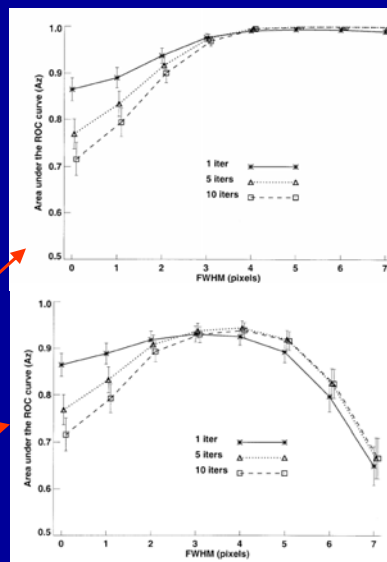
Correlation coef for AUCs: 0.986
CHO performed worse than human

Effect of Quantization

Human Observers



CHO



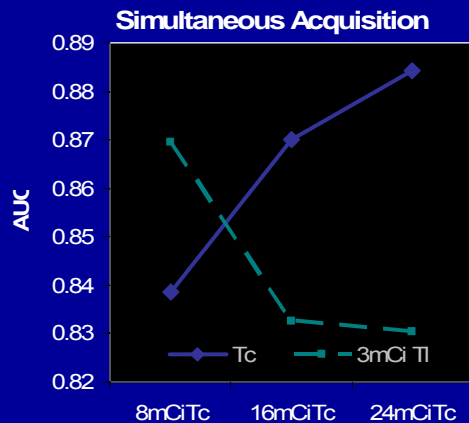
CHO w/o Quantization Noise Model
Correlation Coef=0.604

CHO w/ Quantization Noise Model
Correlation Coef=0.870

From Narayanan 2002

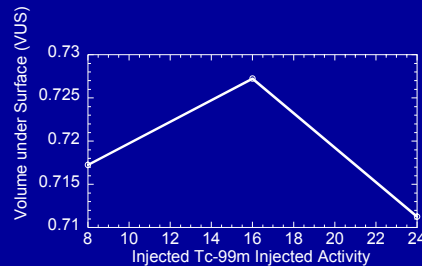
Simultaneous Dual Isotope Myocardial Perfusion SPECT

- Crosstalk:
 - Tc photons corrupt Tl image
 - Tl images corrupt Tc image
- Optimizing relative injected activity (IA) cannot be done using simple detection task



Simultaneous Dual Isotope Myocardial Perfusion SPECT

- Must explicitly consider 3-class nature of task:
 - Use two images
 - To classify patient as
 - Normal
 - Reversible defect
 - Non-reversible defect



	Normal (Class 1)	Reversible (Class 2)	Non-reversible (Class 3)
Stress (^{99m}Tc)	N	D	D
Rest (^{201}Tl)	N	N	D

Example 2 Hepatic SPECT

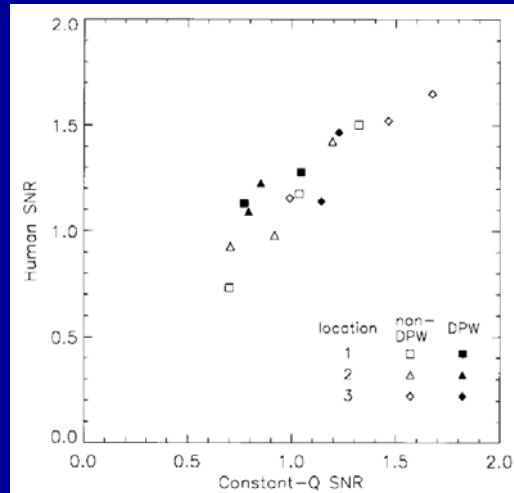
- Gifford 2000
- Task: SKE, BKE (ROC)
- Object Model: Zubal phantom, 3 spherical tumors
- Imaging System Model: MC Simulation
- Observer Model
 - CHO
 - Constant Q w/4 channels
 - D.O.G. w/ 3 channels
 - Ensemble training
 - Explored several combinations of channel parameters
- FOM: CHO SNR

Results

Correlation with Human Observers

- Rank correlation
 - Constant Q: 0.92
 - D.O.G.: 0.84

Comparison of SNR for Human and CHO w/ Constant Q channel model



Example 3

Ga-67 SPECT Imaging

- Gifford 2005
- Task: Detection + Localization (LROC)
- Object
 - MCAT phantom
 - Randomly sampled lesions placed around lymph nodes
- Image Formation
 - Monte Carlo Simulation
 - 2D and 3D reconstruction/processing strategies

Observer Model

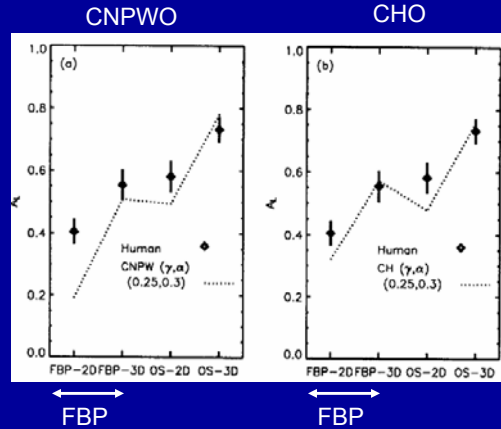
- Used observers with search model including region of uncertainty
- Single and multi-slice observers
- Internal noise appropriate for LROC task
- NPWO
- CNPWO
- CHO
- Constant Q channels with 3 different start frequencies
- Ensemble training (320 images) and testing (100 images)

Figure of Merit

- Test statistics estimated from 100 test images
- A_{LROC} computed using Swenson's ML algorithm

Results Multislice Display

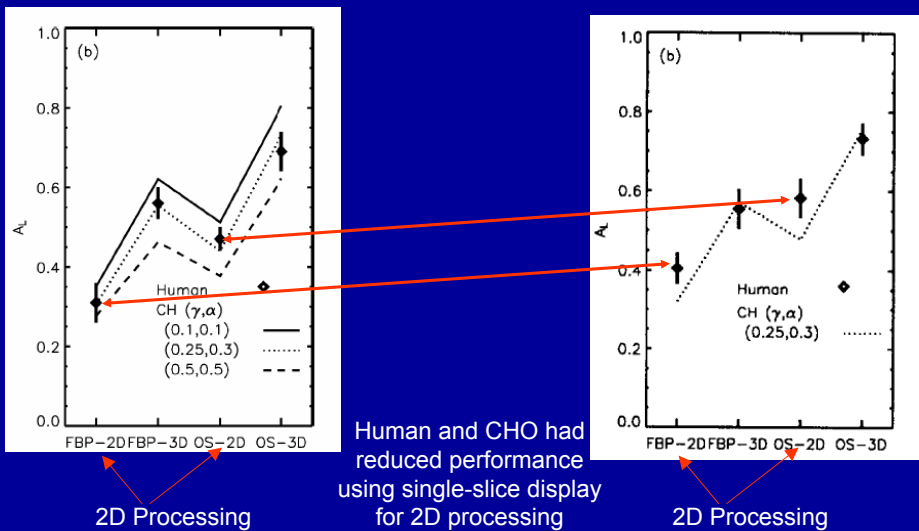
- Both CNPWO and CHO observers predicted rankings of methods
- Good quantitative agreement with appropriate internal noise
- CHO provided better predictions for FBP reconstruction strategies



Results Single vs Multislice Display

Single Slice Display

Multislice Display

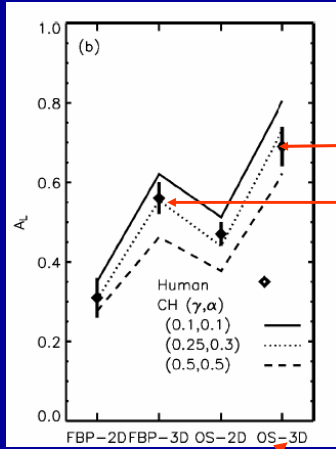


Human and CHO had reduced performance using single-slice display for 2D processing

Results

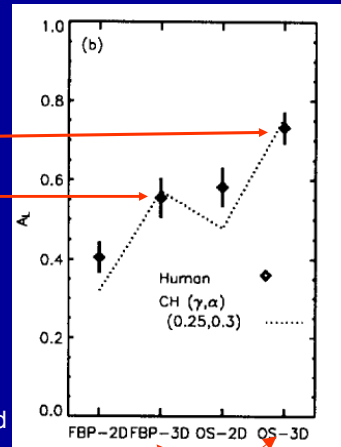
Single vs Multislice Display

Single Slice Display



3D Processing

Multislice Display



3D Processing

Human and CHO had similar performance using single or multi-slice display for 3D processing

Conclusions

- Can model LROC task for both single and multislice observer
- For 3D processing, single-slice observer may be sufficient
- For some algorithms, CNPWO may predict human performance as well as CHO, and is easier to train, for some tasks

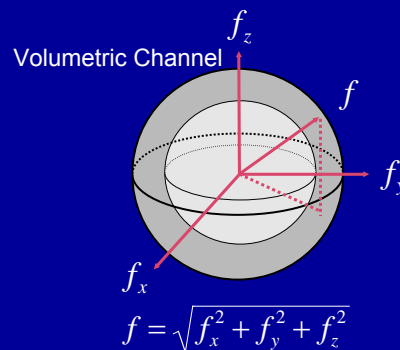
Example 4

2D vs 3D PET Tumor Imaging

- Kim 2004, Lartizen 2004
- Task: Detection (ROC)
- Object:
 - MCAT phantom
 - Multiple lesions per phantom
 - Several sizes and contrasts
- Image Formation
 - Analytic model
 - 2D and 3D acquisition for same activity
 - 2D acquisition with higher activity

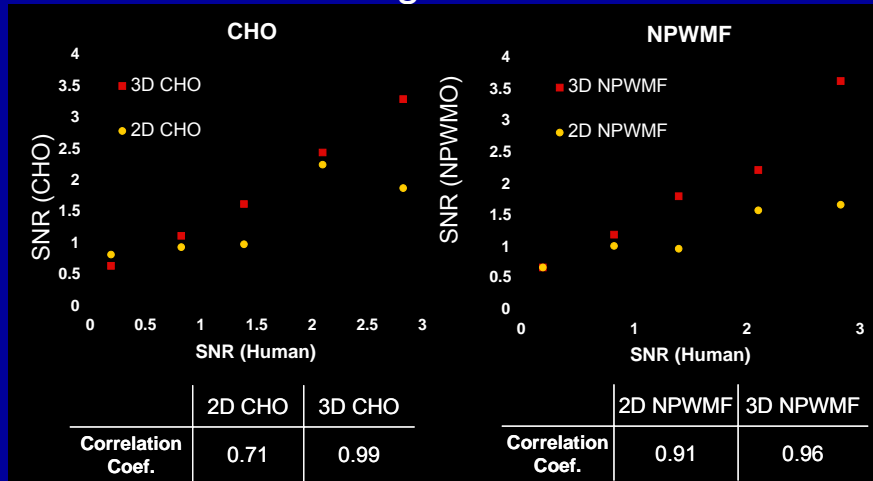
Observer Model

- CHO
 - 2D and volumetric channels
 - Constant Q channel model
 - No internal noise
- NPWO
- Image Contrast
- Ensemble training
- FOMs
 - Detectability index d_A computed from SNR for
 - CHO
 - NPWO
 - Image Contrast



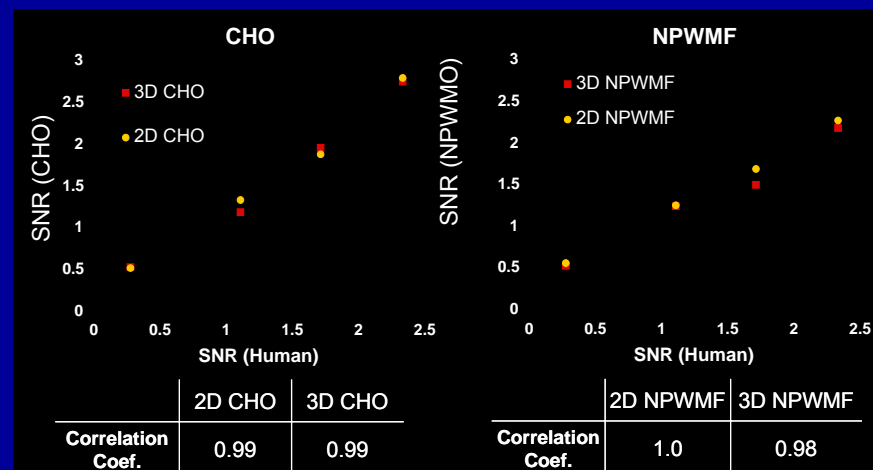
Results Planar vs Volumetric Observer

- No axial smoothing



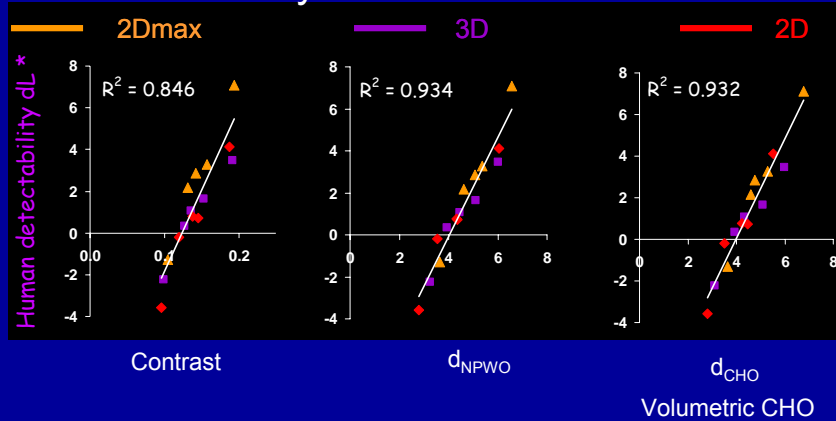
Results Planar vs Volumetric Observer

- With axial smoothing



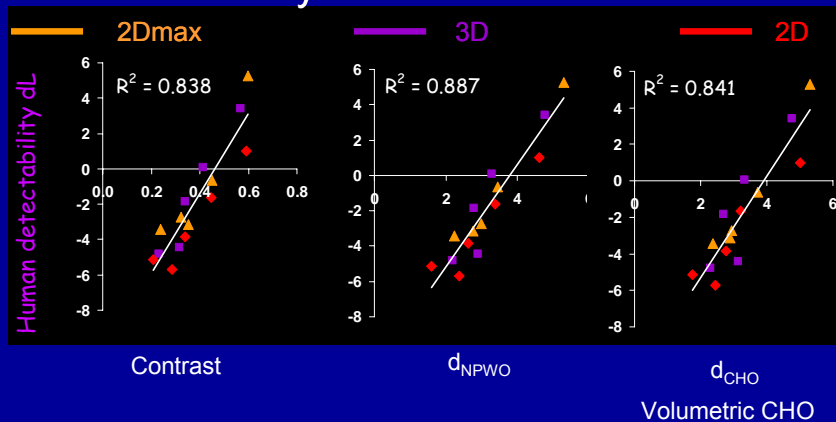
Results Lesions in Lungs

Comparison with results of AFROC human observer study.



Results Lesions in Liver

Comparison with results of AFROC human observer study.



Conclusions

- Volumetric (multi-slice) observer needed when there is only 2-D processing
- CHO performed poorly in soft tissue
 - Perhaps due to presence of multiple lesions
- Contrast did not work well in lungs or liver
- NPWO worked well in both tissues

Example 5

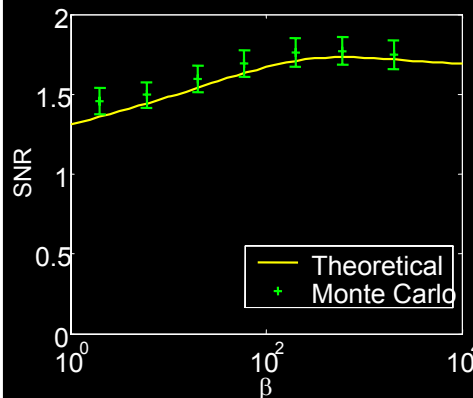
Optimization of Penalty Parameters

- J.Y. Qi 2004, 2006a, 2006b
- Task: Detection (ROC)
- Object Model
 - Torso w/ Lumpy Background
 - Spherical lesions with varying size and position
- Image Formation
 - Analytic 2D simulation
 - Penalized likelihood reconstruction

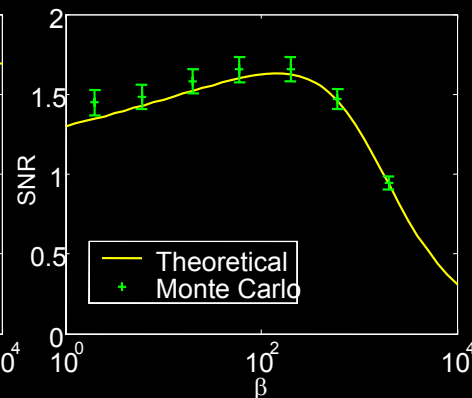
Observer Model

- CHO
- Channel Model
 - SQR and D.O.G. Channels
- Computed using fast (non ensemble) estimation method
- Estimated from noisy and noise-free images
- F.O.M. CHO SNR

Comparison of Fast and Ensemble Estimation of CHO SNR



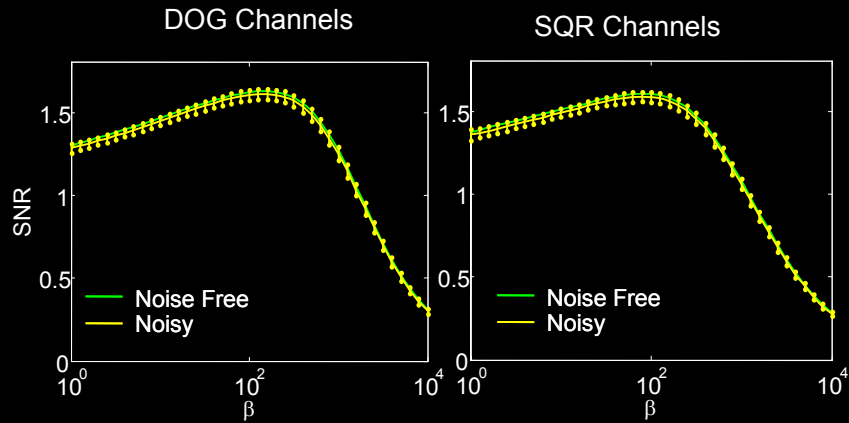
Internal Noise $\sigma^2 = 0$



Internal Noise $\sigma^2 = 0.005$

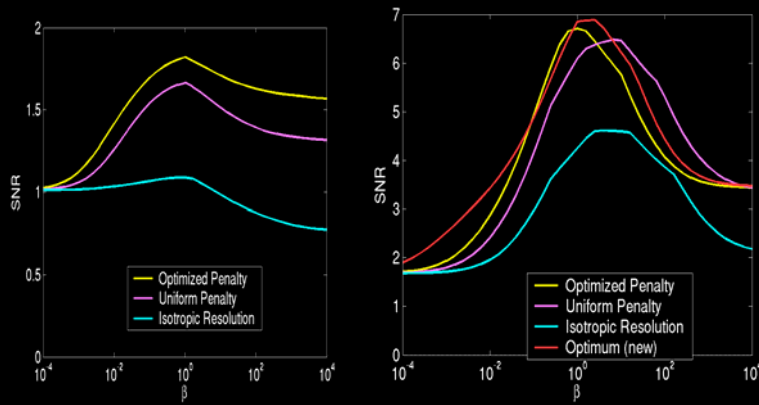
Estimation of FOM from Noisy Images

- Can estimate SNR from noisy images



- From 500 noisy data sets

Optimization of Regularization Parameters



5-mm lesion

15-mm lesion
(with 5-mm lesion penalty functions)

Conclusions

- CHO SNR can be estimated rapidly for penalized likelihood reconstructions
- Can be estimated from noisy data
- Potential to allow for fast optimization of MAP parameters from patient data

Summary

- Model observers have been applied to optimization and evaluation of a wide variety of nuclear medicine imaging problems
- Generally good agreement between human and model observers
- There is a large body of literature describing methods that work
- Must take care to use appropriate task, object, image formation, and observer model to obtain meaningful results
- Validation of observer models still remains important area of research